*Journal of The Electrochemical Society*, **158** (8) H804-H807 (2011)
0013-4651/2011/158(8)/H804/4/$28.00 © The Electrochemical Society

# Enhanced Efficiency of Polymer/ZnO Nanorods Hybrid Solar Cell Sensitized by CdS Quantum Dots

**Lidan Wang,[a,b] Dongxu Zhao,[a,z] Zisheng Su,[a] Binghui Li,[a] Zhenzhong Zhang,[a] and Dezhen Shen[a]**

[a]*Key Laboratory of Excited State Processes, Changchun Institute of Optics, Fine Mechanics and Physics, Chinese Academy of Sciences, Changchun 130033, People's Republic of China*
[b]*Graduate School of Chinese Academy of Sciences, Beijing 100039, People's Republic of China*

The authors demonstrated enhanced efficiency of poly[2-methoxy-5-(2-ethylhexyloxy-*p*phenylenevinylene)]/ZnO nanorods hybrid solar cells sensitized by CdS quantum dots (QDs) prepared by a chemical bath deposition method. A thin ZnO film was adopted to well control the length of the ZnO nanorods and act as a hole blocking layer. An appropriate coating of the CdS QDs on the ZnO nanorods leads to a maximum power conversion efficiency of 0.65%, which was increased 6.5 times compared with the one without using QDs. The dramatically improved efficiency is attributed to the cascade structure formed by the CdS QDs coating, which results in enhanced open-circuit voltage, exciton dissociation efficiency, and charge carriers extraction efficiency.
 [DOI: 10.1149/1.3598171] 

Manuscript submitted March 17, 2011; revised manuscript received April 26, 2011. Published June 10, 2011.

Recently, hybrid solar cells containing a conjugated polymer and an inorganic semiconductor have drawn significant attention because they utilize the high electron mobility inorganic phase to overcome charge-transport limitations associated with organic materials.[1–3] One dimensional nanostructures of inorganic semiconductor have a few special advantages for optoelectronic devices including the large surface area to significantly increase the junction area and the improved carrier confinement in one dimension. Zinc oxide (ZnO) nanorod has been regarded as an excellent semiconductor material for the solar cell due to its high electron mobility as well as the high chemical and thermal stability.[4–6] Various polymer/ZnO nanorods hybrid solar cells have been reported, but the power conversion efficiencies ($\eta_P$) of these devices are still low and need to be further enhanced.[4,5] The key point to increase the efficiency is to improve the photo-absorption properties in the device with enhancing the visible or infrared light absorption. The concept of quantum dots (QDs) sensitization has been considered to be of great promise in increasing the $\eta_P$ of the organic/inorganic hybrid solar cells. Various semiconductor QDs such as CdS,[7,8] CdSe,[9] PbS,[10] PbSe[11] and InP,[12] which absorb light in the visible to infrared region, have been adopted in the hybrid solar cells. The QDs-sensitized ZnO nanostructures based liquid solar cells have been proposed[13] and a more exciting efficiency of 3.26% could be obtained according to the cosensitization by black dye and QDs. But the dye- sensitized solar cells (DSSCs) could not be applied to large areas solar cells comparing to the electrodeposited materials and the encapsulation could be difficult according to the electrolytic solution of the DSSCs. Recently the simple and nontoxic chemical bath deposition (CBD) method of depositing quantum dots were very popular and the photoelectrochemical solar cells sensitized by QDs deposited by this method have been proposed.[14] But few QDs-sensitized organic/ZnO nanorods hybrid solar cells have been reported in the literature. Especially no reports on the effects of different QDs could be found. However, ZnO nanorod synthesized directly on the conductive electrodes usually has a length larger than 0.5 $\mu$m,[15] which leads to a long route for the holes near the cathode traveling to the anode. Consequently, the recombination probability for the dissociated electron hole is increased, resulting in low charge carrier extraction efficiency. On the other hand, the direct contact of the polymer phase to the cathode results in large leakage current. In this paper, ZnO nanorods with appropriate length were synthesized on a thin ZnO film, and a high efficiency CdS QDs sensitized ZnO nanorods/poly[2-methoxy-5-(2-ethylhexyloxy-*p*phenylenevinylene)] (MEH-PPV) hybrid solar cell was designed.

[z] Email: dxzhao2000@yahoo.com.cn

## Experimental

Among the various techniques to obtain one-dimensional ZnO nanostructures, the cost-effective electrodeposition[16] method was used in this work for the nanorods preparation with large areas because of the low-temperature processing, arbitrary substrate shapes, and precise control of the size of nanorods. Primarily, a seed layer of 30 nm was grown by RF magnetron sputtering on cleaned indium tin oxide (ITO) coated glass substrates with a sheet resistance of 25 Ω/□. After that, ZnO nanorods were electrodeposited in 0.005 M $Zn(NO_3)_2$ and 0.005 M hexamethylenetramine aqueous solutions. All depositions were carried out in a configured glass cell at 90°C, in which the ITO substrate, a platinum plate, and an Ag/AgCl electrode in a saturated KCl solution served as the working electrode, the counter electrode and the reference electrode, respectively. All electrodepositions were done at a potential of −0.9 V vs the reference electrode. The durations of the deposition were 20 min. The CdS quantum dots were deposited by CBD method. The CBD process involved dipping the ZnO nanorod in the aqueous solution consisting of 0.1 M $CdCl_2$ and 0.1 M $Na_2S$ for 5 min, respectively. The two-step dipping procedure was considered one CBD cycle. The amount of CdS can be increased by repeating the cycles. MEH-PPV in chloroform (20 mg/ml) was spin coated onto the surface of the CdS QDs/ZnO nanorods structures at 2000 r/min. Films were baked in a vacuum oven for 30 min at 100°C. Then, a thin layer of poly(3,4-ethylenedioxythiophene)-poly(styrenesulfonate) (PEDOT:PSS) was spin-coated on the MEH-PPV film at 2000 r/min and baked in a vacuum oven for 1 h at 120°C. Finally, Au electrode was evaporated onto the device as the top electrode. The field emission scanning electron microscopy (FESEM) measurements were performed by the Hitachi FESEM S-4800. The absorption spectrum was recorded using a Shimadzu UV-3101PC spectrophotometer. The photoresponse of the device was studied using a 150 W Xe lamp, monochromator, a chopper (EG&G 192), and a lock-in amplifier (EG&G 124A). Current-voltage (I-V) characteristics of the devices were measured using a Keithley 2400 source meter connected with a GPIB controller to a computer under dark or one sun illumination (AM1.5, 100 mW/cm$^2$). All the measurements were carried out at room temperature under ambient conditions.

## Results and Discussion

Figure 1 shows the typical field emission scanning electron microscopy (FESEM) images of ZnO nanorod arrays with and without CdS QDs coating. It can be observed that the diameter and the length of the nanorods are in the ranges of 40–80 and 200–300 nm, respectively. The short length of ZnO nanorods is beneficial to the insert of the thin ZnO film, and the detail growth mechanism is under investigation. The surface of ZnO nanorods was partially

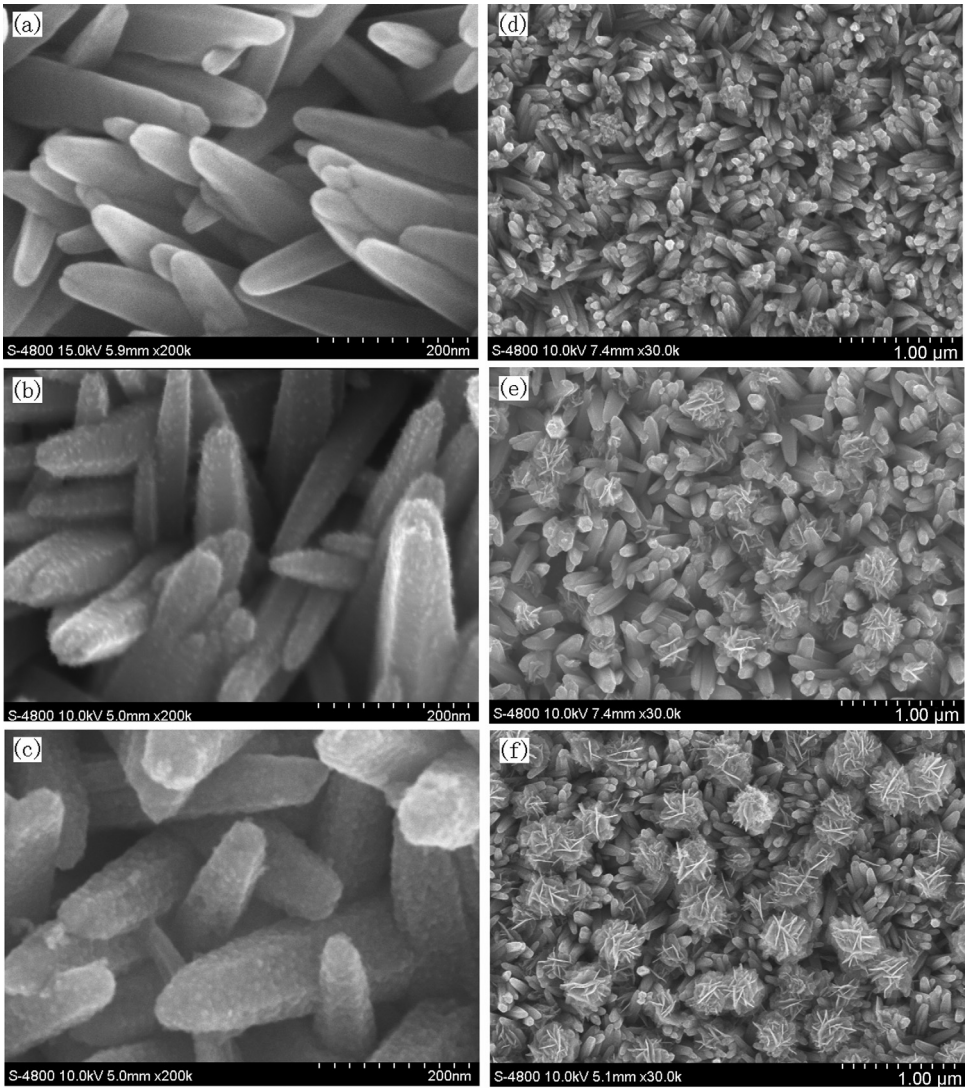


**Figure 1.** (a–c) The FESEM image of ZnO nanorods as-prepared and CdS QDs coated ZnO nanorod arrays with 3 and 6 CBD cycles. The scale bar is 200 nm. (d–f) The FESEM image of CdS QDs coated ZnO nanorod arrays with 6, 9, and 12 CBD cycles. The scale bar is 1 $\mu$m.

coated by CdS QDs with the diameter of 2–5 nm at 3 CBD cycles. The CdS QDs diameter increased to 6–10 nm with 6 CBD cycles and the coverage of the CdS QDs on the ZnO nanorods was increased. Moreover, some small CdS flowers could be found on the ZnO nanorods, as shown in Fig. 1d. And the diameter and amounts of CdS flowers increased with further increasing CBD cycles.

Figure 2 shows the absorption spectra of ZnO nanorods, CdS QDs coated ZnO nanorod arrays with different CBD cycles, and MEH-PPV. As shown in the figure, ZnO nanorods could only absorb the high energy light with the wavelength shorter than 370 nm. With the CdS coating the UV optical absorption edges of ZnO/CdS hybrid nanostructures are red-shifted to the long-wavelength side gradually with increasing the CBD growth circles. And the absorption for the visible region is also increased a lot. It can be found in the figure that the absorption for the wavelength in the region of 370–550 nm increases with CdS CBD cycles as expected. The red-shift of the UV absorption edge for the ZnO/CdS hybrid nanostructures was observed for the S-doped ZnO,[17] which was attributed to the formation localized band edge states due to change exchange and structural relaxation.[18] In our experiment, the S element could incorporated to the ZnO lattices during the CBD growth process, which induces the narrowing of the bandgap. The red-shift of the UV absorption edge for the ZnO/CdS hybrid nanostructures can also ascribed to the gradually increasing size of the QDs due to the absorption edge would to be blue-shifted with the decreasing size of

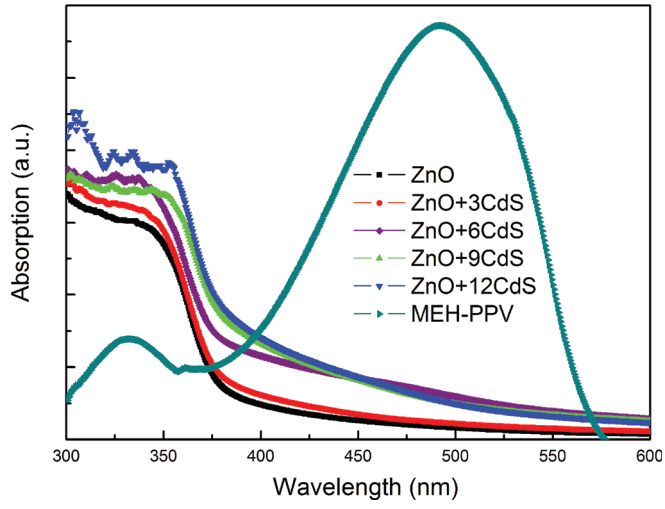


**Figure 2.** (Color online) The absorption spectra of ZnO nanorods, the ZnO nanorods with different cycles of CBD-CdS QDs and MEH-PPV.

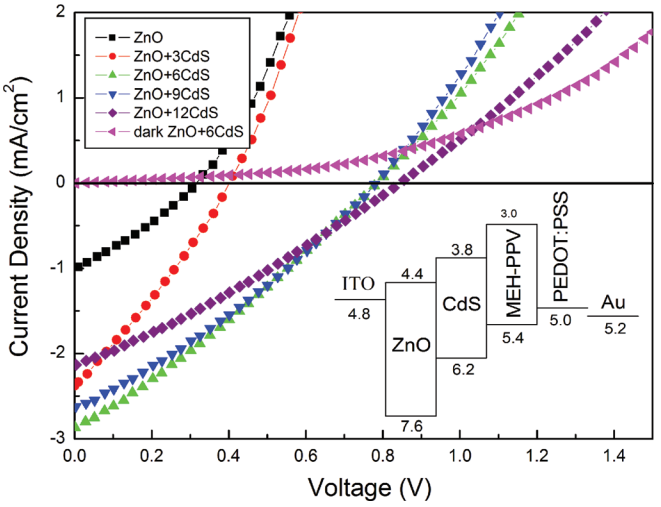


**Figure 3.** (Color online) The I-V characteristics of the MEH-PPV/ZnO solar cell and the solar cells sensitized by the CdS quantum dots under illumination of 1.5 sun (100mW $cm^{-2}$) and the I-V characteristics of the solar cell after introduction of CdS quantum dots using 6 CBD cycles in the dark. The inset shows the band structure for polymer/ZnO solar cell sensitized by CdS QDs.

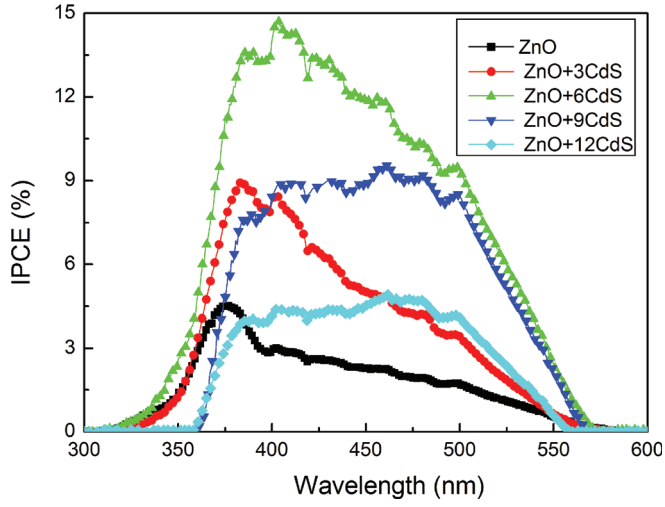


**Figure 4.** (Color online) The IPCE spectra of the MEH-PPV/ZnO solar cell and the solar cells sensitized by different CdS QDs.

the QDs according to the quantum effect. While the MEH-PPV showed a predominant absorption band in 400–570 nm which was the same with the reports of others[19] and has contribution to the absorption of the visible region.

Figure 3 shows the I-V characteristics of MEH-PPV/ZnO solar cells with and without the CdS QDs sensitization under illumination (AM1.5, 100 mW/$cm^2$) and under dark. Detail parameters of the solar cells extracted from the I-V characteristics were listed in Table I. The MEH-PPV/ZnO solar cell showed a short-circuit current density ($J_{SC}$), an open-circuit voltage ($V_{OC}$), a fill factor ($FF$), and a $\eta_P$ of 0.98 mA/$cm^2$, 0.32 V, 0.30, and 0.10%, respectively. The $J_{SC}$ of the CdS QDs sensitized solar cells increased with the CBD cycles, and a maximum $J_{SC}$ of 2.87 mA/$cm^2$ was obtained with 6 CBD cycles. Further increase of the CBD cycles resulted in a decrease of $J_{SC}$. Meanwhile, the $V_{OC}$ of the CdS QDs sensitized solar cells increased with the CBD cycles, and it almost saturated after 6 CBD cycles. However, the $FF$ was not high and did not show much difference with different CBD cycles. The longer nanorods would lead to the thicker polymer layer in the solar cell and would limit the transmission of the carriers. And the inappropriate length of the nanorods would increase the recombination probability for the dissociated electron hole, resulting in low charge carrier extraction efficiency. The low fill factor could be improved by more appropriate nanostructures. As a result, the CdS QDs sensitized solar cell with 6 CBD cycles showed a maximum $\eta_P$ of 0.65%, which was increased 6.5 times compared with the one without CdS QDs.

The band structure of the CdS QDs sensitized MEH-PPV/ZnO solar cells formed a cascade energy alignment,[8,19] as shown in the inset of Fig. 3. The $V_{OC}$ was reported to track with the energy difference between the highest occupied molecular orbital (HOMO) level of the donor and the lowest unoccupied molecular orbital (LUMO) level of conduction band edge of the acceptor.[4,20] From the band diagram, the $V_{OC}$ increasing in the CdS QDs sensitized MEH-PPV/ZnO solar cells can be reasonable understood because the conduction band of CdS was higher (lower electron affinity) than that of ZnO, and it would saturate after the whole surface of the ZnO nanorods are coated with CdS QDs. Besides, the passivation of the surface states of the ZnO nanorods by the CdS coating would lead recombination decreasing or charge trapping and the cascade structure formed charge carrier recombination barrier could also result in $V_{OC}$ improvement.

**Table I. Parameters of polymer/ZnO solar cells sensitized by various CdS quantum dots.**

| CBD cycle | $J_{SC}$(mA/$cm^2$) | $V_{OC}$(V) | $FF$ | $\eta_P$(%) |
|---|---|---|---|---|
| 0 | 0.98 | 0.32 | 0.30 | 0.10 |
| 3 | 2.55 | 0.41 | 0.29 | 0.28 |
| 6 | 2.87 | 0.78 | 0.29 | 0.65 |
| 9 | 2.62 | 0.79 | 0.30 | 0.62 |
| 12 | 2.13 | 0.85 | 0.28 | 0.52 |

Figure 4 shows the incident photo to charge carrier generation efficiency (IPCE) spectra of the MEH-PPV/ZnO and the CdS QDs sensitized MEH-PPV/ZnO solar cells illuminated from the ITO glass side. The IPCE was monitored to compare the photoresponse using the equation[21]

$$IPCE(\%) = \frac{1240 \cdot I_{SC}(A)}{Pi(W) \cdot \lambda(nm)} \cdot 100\% \quad [1]$$

As shown in the figure, the IPCE spectrum of the MEH-PPV/ZnO cell showed a peak at about 375 nm, which was ascribed to the absorption of ZnO nanorod array, and the response in the visible region was quite low. This result indicated that the photogenerated MEH-PPV excitons could not be dissociated efficiently and/or the charge carriers could not be extracted effectively in this device. With the CdS QDs being sandwiched in ZnO nanorods and MEH-PPV, the response of the cells increased in the whole wavelength region, and a maximum IPCE of 14.7% was obtained at 405 nm with 6 CBD cycles. The IPCE enhancement could be attributed the cascade band structure formed with the CdS QDs coating and higher carrier mobility of inorganic semiconductors. Such a cascade structure ensured excitons formed in any of the three materials, e.g., ZnO nanorods, CdS QDs, and MEH-PPV, could be dissociated into a free electron and hole at the ZnO/CdS and CdS/MEH-PPV interfaces. Then the electrons and holes would transport through ZnO and MEH-PPV to the ITO and Au electrodes, respectively. The cascade structure would restrict electron and hole recombination when transporting in the active layers and hence leaded to a high charge carrier extraction efficiency. Moreover, the ZnO seed layer would avoid the direct contact between MEH-PPV and the ITO electrode and forbid the hole leakage to the ITO electrode. These factors, combining with the high $V_{OC}$, brought a high $\eta_P$ of 0.65% in the 6 CBD cycles CdS QDs sensitized MEH-PPV/ZnO solar cell. When the CBD cycles further increased, the IPCE in the whole wavelength region was decreased, and the response in the visible region became the dominant component. As shown in Fig. 1, the diameter of CdS QDs

was increased and the CdS flowers were formed with increasing CBD cycle, and such CdS flowers might limit the infiltrate of MEH-PPV into the ZnO nanorod arrays. Both these factors could reduce the direct contact area between the inorganic semiconductors, e.g., ZnO nanorods and CdS QDs, and MEH-PPV, which reduced the charge transfer and exciton dissociation efficiencies. Besides, the growth of CdS QDs was an erosive process for the ZnO nanorods, which could decreased the IPCE in the ultraviolet region due to the reduce of ZnO amount.[22] The above effects resulted in the decrease of the $J_{SC}$ values and hence $\eta_P$.

## Conclusions

In summary, an efficient CdS QDs sensitized MEH-PPV/ZnO nanorods hybrid solar cell with appropriate ZnO nanorod length was demonstrated. A maximum $\eta_P$ of 0.65% was demonstrated, which was 6.5 time higher than the one without CdS QDs. The dramatically improved efficiency was attributed to the cascade structure formed by the CdS QDs coating, which results in enhanced $V_{OC}$, exciton dissociation efficiency, and charge carriers extraction efficiency. It is expected that by using the suitable QDs to enhance the visible to infrared absorption, the efficiency of the hybrid solar cells could be further improved.

## Acknowledgments

This work is supported by the Key Project of National Natural Science Foundation of China under Grant No. 50532050, the "973" program under Grant No. 2006CB604906, the CAS Innovation Program, the National Natural Science Foundation of China under Grant No. 60506014 and 11004187.

## References

1. W. J. E. Beek, M. M. Wienk, and R. A. J. Janssen, *Adv. Mater.*, **16**, 1009 (2004).
2. S. Rani, P. Suri, P. K. Shishodia, and R. M. Mehra, *Sol. Energy Mater. Sol. Cells.*, **92**, 1639 (2008).
3. Y.-J. Lee and Y.-S. Lo, *Adv. Func. Mater.*, **19**, 604 (2009).
4. M. H. Huang, S. Mao, H. Feick, H. Yan, Y. Wu, H. Kind, E. Weber, R. Russo, and P. Yang, *Science*, **292**, 1897 (2001).
5. C. S. Lao, M.-C. Park, Q. Kuang, Y. Deng, A. K. Sood, D. L. Polla, and Z. L. Wang, *J. Am. Chem. Soc.*, **129**, 12096 (2007).
6. L. E. Greene, M. Law, J. Goldberger, F. Kim, J. C. Johnson, Y. Zhang, R. J. Saykally, and P. Yang. *Chem. Int. Ed.*, **42**, 3031 (2003).
7. S.-C. Lin, Y.-L. Lee, C.-H. Chang, Y.-J. Shen, and Y.-M. Yang, *Appl. Phys. Lett.*, **90**, 143517 (2007).
8. H. J. Lee, H. C. Leventis, S.-J. Moon, P. Chen, S. Ito, S. A. Haque, T. Torres, F. Nuesch, T. Geiger, S. M. Zakeeruddin, et al., *Adv. Func. Mater.* **19**, 2735 (2009).
9. I. Robel, V. Subramanian, M. Kuno, and P. V. Kamat, *J. Am. Chem. Soc.*, **128**, 2385 (2006).
10. P. Hoyer and R. Konenkamp, *Appl. Phys. Lett.* **66**, 349 (1995).
11. K. S. Leschkies, A. G. Jacobs, D. J. Norris, and E. S. Aydil, *Appl. Phys. Lett.*, **95**, 193103 (2009).
12. A. Zaban, O. I. Mićić, B. A. Gregg, and A. J. Nozik, *Langmuir*, **14**, 3153 (1998).
13. J. Chen, D. W. Zhao, W. Lei, and X. W. Sun, *IEEE J. Sel. Top. Quantum Electron.*, **16**, 1607 (2010).
14. M. Thambidurai, N. Muthukumarasamy, N. S. Arul, S. Agilan, and R. Balasundaraprabhu, *J. Nanopart. Res.*, **4**, 1 (2011).
15. Y. Y. Lin, C. W. Chen, W. C. Yen, W. F. Su, C. H. Ku, and J. J. Wu, *Appl. Phys. Lett.* **92**, 233301 (2008).
16. L. Wang, D. Zhao, Z. Su, F. Fang, B. Li, Z. Zhang, D. Shen, and X. Wang, *Org. Electron.* **11**, 1318 (2010).
17. Y. Z. Yoo, Z. W. Jin, T. Chikyow, T. Fukumura, M. Kawasaki, and H. Koinuma, *Appl. Phys. Lett.*, **81**, 3798 (2002).
18. J. E. Bernard and A. Zunger, *Phys. Rev. B*, **36**, 3199 (1987).
19. M. Lira-Cantu and F. C. Krebs, *Sol. Energy Mater. Sol. Cells.*, **90**, 2076 (2006).
20. D. C. Olson, S. E. Shaheen, M. S. White, W. J. Mitchell, M. F. A. M. van Hest, R. T. Collins, and D. S. Ginley, *Adv. Func. Mater.* **17**, 264 (2007).
21. D. R. Baker and P. V. Kamat, *Adv. Func. Mater.* **19**, 805 (2009).
22. Y. Tak, S. J. Hong, J. S. Lee, and K. Yong, *Cryst. Growth Des.*, **9**, 2627(2009).